Kinematically complete measurement of the $(\pi^{\pm},\pi^{\pm}p)$ reaction on ^{12}C at 220 MeV

J. A. Faucett,* B. E. Wood,† and D. K. McDaniels
University of Oregon, Eugene, Oregon 97403

P. A. M. Gram, M. E. Hamm,‡ and M. A. Oothoudt
Los Alamos National Laboratory, Los Alamos, New Mexico 87545

C. A. Goulding†
University of Texas at Austin, Austin, Texas 78712

L. W. Swenson, K. S. Krane, and A. W. Stetz
Oregon State University, Corvallis, Oregon 97331

H. S. Plendl and J. Norton
Florida State University, Tallahassee, Florida 32306

H. Funsten and D. Joyce
College of William and Mary, Williamsburg, Virginia 23185
(Received 21 February 1984; revised manuscript received 14 August 1984)

The $^{12}C(\pi^{\pm},\pi^{\pm}p)$ reactions were studied at $T_{\pi}=220$ MeV. The final particles were detected both separately and in coincidence and their momenta were measured. Calculation of the excitation energy of the residual nucleus allowed clear separation of events where an outer proton was removed. The data provide detailed evidence confirming the quasielastic picture of pion knockout reactions. Evidence for this derives from the agreement between the peak energies found in the coincidence spectra and those found in inclusive spectra, from analysis of angular distributions, and from the location of peaks found in missing mass spectra. The coincidence cross section is found to account for about half of the $(\pi^{+},\pi^{+\prime})$ reaction, and about half of this in turn corresponds to quasifree knockout of the outer shell protons. Secondary processes in the $(\pi^{-},\pi^{-}p)$ reaction are found to play a much more important role than in the $(\pi^{+},\pi^{+}p)$ reaction.

I. INTRODUCTION

Comprehension of the dynamics of pion-nucleus reactions would be greatly aided by detailed experimental information on the major reaction processes. We report here a measurement of the exclusive pion-induced proton knockout reaction from ^{12}C at an incident pion energy of 220 MeV, just above the (3,3) resonance, for a wide range of kinematic conditions. These data comprise measurements of the energy and angle of both scattered particles detected in coincidence, as well as information which can be deduced on the fate of the residual nucleus. Most previously published studies of pion induced knockout reactions have identified only the residual nucleus by activation or gamma ray detection techniques,[1-4] have detected only one of either the scattered pion or nucleon,[5-8] or have not measured both momenta.[9] Some earlier coincidence $(\pi,\pi'p)$ experiments[10,11] were carried out under restricted kinematic conditions. The results presented here demonstrate that defining the kinematics of a proton knockout reaction yields spectra in which the background seen to either side of the quasifree peak in inclusive observations (presumably due to final state interactions and other reactions) has been eliminated. The information we obtain on the state of the residual nucleus allows the separation of events where an outer shell proton was removed from other possibilities. This separation helps exhibit the extent to which the knockout reaction is a quasifree process.

II. EXPERIMENTAL DETAILS

The experiment was performed at the Clinton P. Anderson Meson Physics Facility (LAMPF) using pions from the P^3 East channel with a kinetic energy of 220 MeV. These were focused to a spot 2 cm diam on a natural carbon target (98.9% ^{12}C) with a thickness of 226 mg/cm^2. Relative measurement of the incident pion flux was done with an argon-filled ionization chamber of 6 cm thickness placed upstream from the target. The outgoing pions and protons were detected in coincidence. In addition, fixed fractions of each of the pion and proton singles rates were accumulated.

The experimental arrangement is shown in Fig. 1.

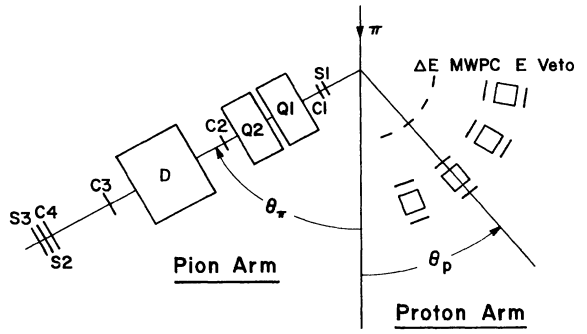

FIG. 1. Schematic of the experimental arrangement. (Figure not to scale.)

Pions were detected with the Large Acceptance Spectrometer (LAS) developed by the authors of Ref. 6 (see also Ref. 12). LAS consists of a quadrupole doublet followed by a dipole with a 45° vertical bend of the central trajectory. The transverse coordinates of a particle traversing the spectrometer were measured by the four multiwire proportional chambers (MWPC's) $C1$–$C4$. A pion event was defined by signals in coincidence from the scintillators $S1$, $S2$, and $S3$. The pion's momentum and point of origin in the target were calculated from algorithms of the wire chamber coordinates. In this analysis of the data, the solid angle was limited to 15 msr. Spectrometer events were accepted for further analysis on the basis of time-of-flight and pulse height information from the scintillators and were rejected if there were missing or multiple hits in any of the wire chambers. Since the momentum could be calculated from coordinate information from three of the four chambers, a comparison between the momentum calculated from chambers 1, 3, and 4 and chambers 2, 3, and 4 helped to reject events due to a pion which decayed or scattered within the spectrometer. It was further required that the calculated pion momentum, p_π, be in the range where $(p_\pi - p_0)/p_0$ is from -12% to 32% (p_0 is the spectrometer central momentum). A Monte Carlo simulation showed that about 3% of the remaining events corresponded to pions which had decayed within the spectrometer. Energy losses of the pion in the target and spectrometer were negligible.

The proton detector consisted of four telescopes, each having a 15 cm wide $\times$15.75 cm deep $\times$32.25 cm high scintillator viewed from each end via light pipes by 12.70 cm phototubes. The signals from each end were added and used to calculate the proton energy. Position information available from a delay-line MWPC placed in front of each scintillator was used when necessary to compensate for a 6% variation in the light collection efficiency with position. A thin "ΔE" scintillator was used in conjunction with each of the larger scintillators for particle identification while thin veto counters behind the E counters rejected particles not stopped in the E counters. Corrections for energy losses in the target telescope were included in the determination of the proton energy. Protons with energies greater than 35 MeV and less than 145 MeV were detectable. The four telescopes, which moved together as a unit, were separated by 20°; each subtended 7° in the horizontal plane and 17° in the vertical plane.

Energy calibration for both pions and protons as well as the spectrometer acceptance function were obtained by observing the scattering of the respective particles to a small angle from a very thin lead target. The resolution in pion energy was 1.5% FWHM and that in the proton energy was about 5% at 100 MeV. Absolute normalization of the measured cross sections was achieved by scattering pions from the hydrogen in a scintillator target and comparing them with the pion-nucleon cross sections calculated from phase shifts.[13] The total absolute uncertainty is estimated to be $\pm 12\%$ for the coincidence cross sections. The largest sources of uncertainty are the monitor instability ($\pm 6\%$) and the uncertainty in the proton wire chamber efficiency ($\pm 6\%$).

Measurements were made at pion angles of 61°, 81°, 105°, and 127° for incident π^+ and at 81° for incident π^-. Data in one to four momentum bites were accumulated at each angle. Cross sections were calculated by correcting for the acceptance and summing together the several corrected histograms obtained at each pion angle. The proton detector was set with the first telescope at 20° and also at 15° or 30° for certain pion angles. It was impossible to set a scintillator closer to the beam than 15° because of the counting rate encountered. These proton telescope angles were chosen to sample the proton distributions in the angular region where free protons elastically scattered by pions arriving at the selected pion angle would appear. In the 127° case, half of the angular correlation peak occurred at proton angles less than 15°. The uncertainty in the relative normalizations between data accumulated for different spectrometer momentum settings was found to be $\pm 15\%$. Error bars shown on the figures are due only to statistics.

III. RESULTS

A. Energy spectra

The inclusive and coincidence pion energy spectra for incident π^+ are displayed in Fig. 2 for each pion angle. (Tabulation of the experimental results are given elsewhere.[14]) "Inclusive" here refers to those events where only a final pion was detected. The position of the peak in the inclusive cross sections is slightly below that for elastic kinematics, the difference being largest in the 81° data. This tendency is also seen in the data of Ref. 9: The inclusive cross section (which was measured at a greater number of angles than in the present experiment) shows the peak position approaching the elastic kinematics energy for forward and back angles. For the present experiment, the width of the coincidence peak is about the same at all the pion angles. At each angle the peak is near the same energy as in the inclusive cross section. This peak is largest for proton angles near the angle corresponding to elastic πp kinematics and falls off considerably or is not seen at all at other angles (see Table I). At the forward angles, the elastic and lower excited states are visible in the inclusive spectra, but are not resolved. The

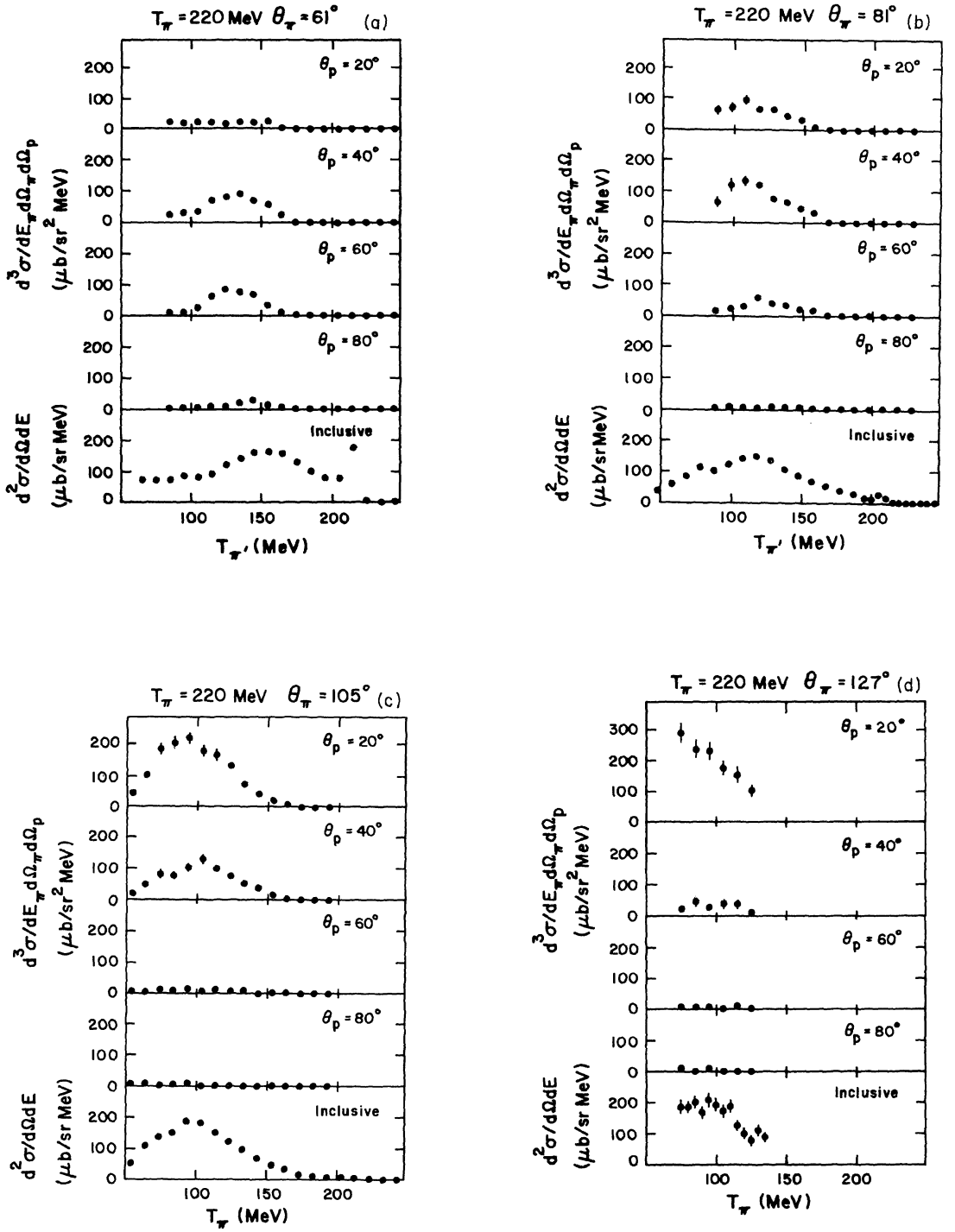

FIG. 2. The pion energy spectra obtained for 220 MeV π^+ incident on ^{12}C for θ_π equal to (a) 61°, (b) 81°, (c) 105°, and (d) 127°. In each case, the top four spectra are for coincidence events with the angle of the telescope in which the proton was detected indicated and the inclusive reaction cross section is shown in the bottom spectrum. Note that the horizontal scale has a nonzero origin and that the vertical scale units of the inclusive spectra differ from that of the coincidence spectra. The coincidence spectra at the higher pion energies are affected by the proton detector low energy cutoff at T_p=45 MeV. This effect sets in between T_π=150 MeV (θ_p=80°) and T_π=160 MeV (θ_p=20°).

TABLE I. Elastic kinematics in the laboratory frame corresponding to the conditions under which the present data were taken. The fifth column is the momentum transfer.

θ_π (deg)	$T_{\pi'}$ (MeV)	θ_p (deg)	T_p (MeV)	Δp (MeV/c^2)
61	169.5	50.7	50.5	129.0
81	145.3	40.0	74.7	162.6
105	120.9	28.7	99.1	193.6
127	104.6	19.5	115.4	213.4

quasielastic peaks in the 61° coincidence spectra appear to be shifted to lower pion energies than the peak in the inclusive cross section. This is an experimental artifact due to the low energy cutoff at about 45 MeV in the proton detectors.

By contrast with the pion energy spectra, the inclusive proton cross sections are found to be nearly featureless, generally decreasing with increasing proton energy. The yield of low energy protons is mainly due to nonquasielastic processes which dominate the quasielastic peak. Figure 3 shows the coincidence proton energy spectra for a pion scattering angle of 81°. Now the quasielastic peak can be clearly distinguished. For the protons, the peak position is slightly above the elastic kinematics energy. The difference here is least for the 81° data, in contrast to the pion coincidence energy spectra. The widths of the proton quasielastic peaks are about the same as those of the pions (in momentum), as would be expected if the pion indeed transfers momentum to a single nucleon.

Denoting the pion momentum and total energy by $\vec{p}_\pi$ and E_π and the corresponding quantities for the proton and residual nucleus by the subscripts "p" and "R", respectively, the residual nucleus momentum is given by conservation of momentum:

$$\vec{p}\,'_R = \vec{p}_\pi - \vec{p}\,'_\pi - \vec{p}\,'_p \ ,$$

where the quantities before (after) the reaction are unprimed (primed). The missing mass corresponds to the excitation energy of the residual nucleus. This is given by the separation energy of the proton, E_S, less the separation energy of the least bound proton, E_B. E_S is given by the conservation of energy:

$$E_S = E_\pi - E'_\pi - E'_p - E'_R \ ,$$

where $E'^2_R = \vec{p}\,'^2_R c^2 + m^2_R c^4$, m_R being the ground state mass of the residual nucleus. For ^{12}C, E_B is 16.0 MeV. The missing mass spectra for incident π^+ are shown in Fig. 4. These spectra can be divided into two regions: the region below about 10 MeV has in most cases a peak centered near zero missing mass; this feature is strongest near the proton angle corresponding to elastic kinematics. This region corresponds to the events where the nucleus is left in its ground state or a low excited state, as one would expect if a $1p$ shell proton had been knocked out with no major final state interactions. More than half of the observed events for near-elastic kinematics fall in this region. The events in the region above 10 MeV correspond to either proton knockout from the $1s$ shell, pion multiple

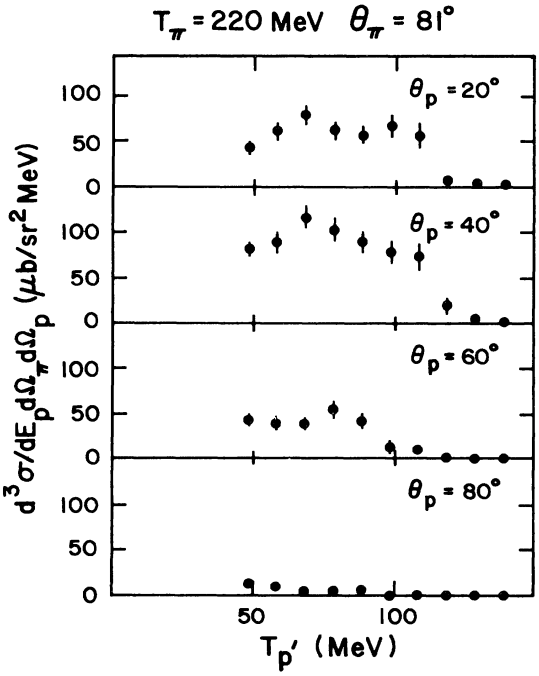

FIG. 3. The proton energy spectra obtained for 220 MeV π^+ incident on ^{12}C for $\theta_\pi = 81°$. These are for coincidence events with the angle of the telescope in which the proton was detected indicated.

scattering, or nucleon final state interactions. The separation energy for $1s$ protons measured by (e,ep) and (p,2p) experiments yield a knockout excitation energy of around 22 MeV and a peak width of about 20 MeV.

The corresponding (π^-,π^-p) cross sections measured in this experiment are shown in Figs. 5–7. The energy and missing mass spectra show features similar to those seen in the π^+ case. These data are limited to $\theta_\pi = 81°$ only, and they represent only two settings of the spectrometer and have rather poor statistics; therefore little more can be said about the systematics of the data. The main utility of the data is the comparison, presented later, with the positive pion data at the same angle.

B. Angular distributions

The angular distributions of the integrated cross sections for incident $\pi^\pm$ are shown in Fig. 8. These were obtained by integrating over the pion coincidence spectra and adding the estimates of the cross section not directly measured because of detector energy cutoffs. These estimates were obtained by linear extrapolation of the pion coincidence spectra to zero cross section at zero energy. For several of the more incomplete spectra an inflection point in the extrapolation was deemed appropriate since the energy cutoff was near a maximum in the data. The effect of the proton detector energy cutoff was compensated for by including estimates of the missing cross sections obtained from a similar extrapolation of the proton coincidence spectra. The peaking of the yield near the elastic kinematics (shown by arrows) is apparent in Fig.

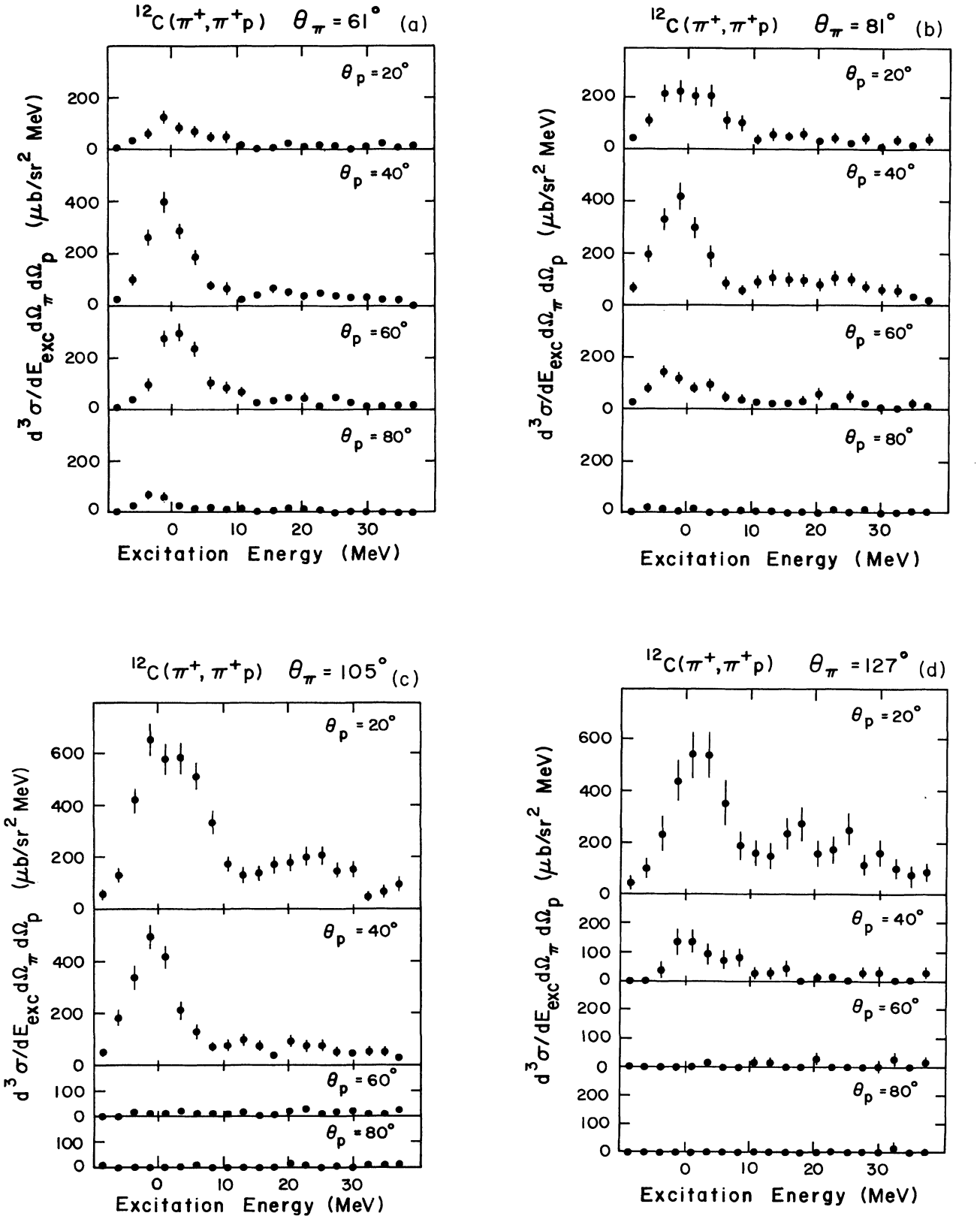

FIG. 4. The missing mass spectra obtained for 220 MeV π^+ incident on ^{12}C for θ_π equal to (a) 61°, (b) 81°, (c) 105°, and (d) 127°.

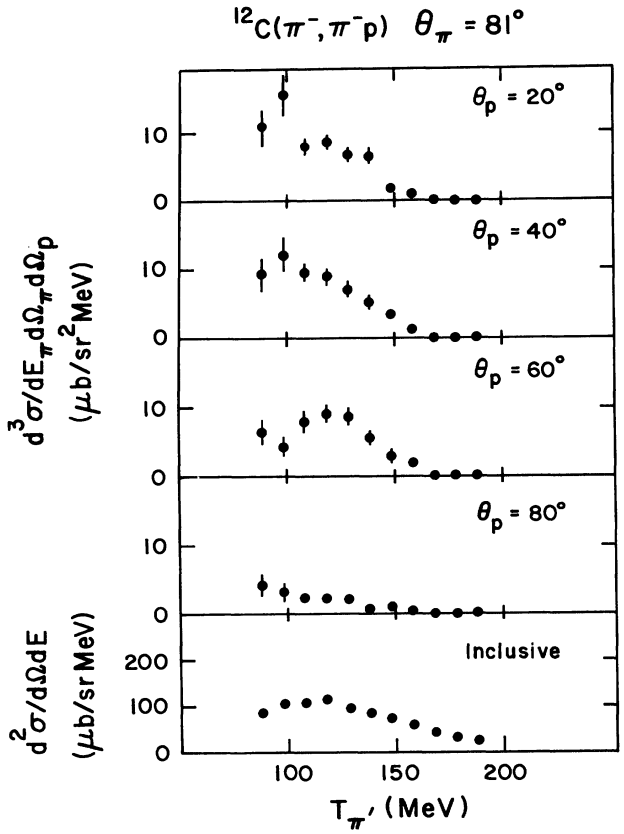

FIG. 5. The pion energy spectra obtained for 220 MeV π^- incident on ^{12}C for $\theta_\pi = 81°$. See the caption for Fig. 2.

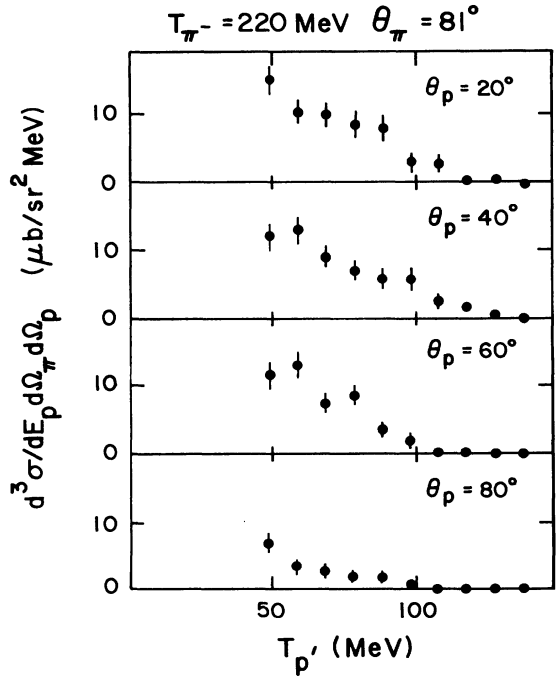

FIG. 6. The proton energy spectra obtained for 220 MeV π^- incident on ^{12}C for $\theta_\pi = 81°$. These are for coincidence events with the angle of the telescope in which the proton was detected indicated.

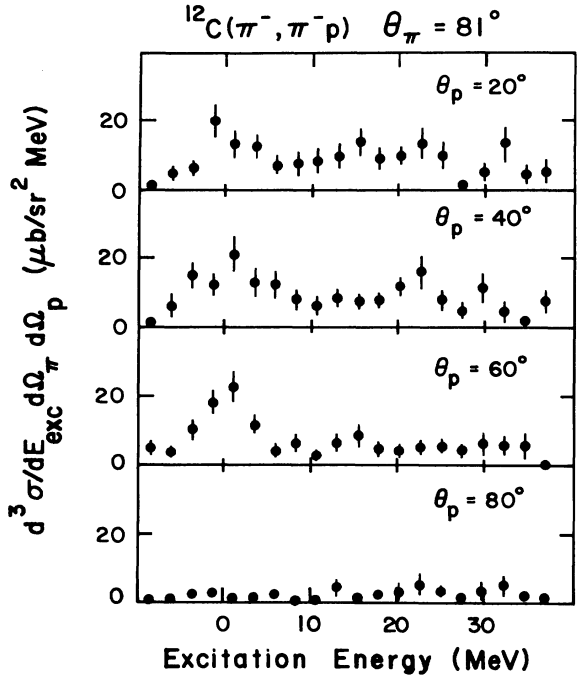

FIG. 7. The missing mass spectra obtained for 220 MeV π^- incident on ^{12}C for $\theta_\pi = 81°$.

8(a), but in Fig. 8(b), which shows the same cross section for incident π^-, an angular distribution peak is not evident.

The yield is expected to have a roughly Gaussian distribution in the azimuthal angle.[9] Reference 9 also shows that the azimuthal distribution has about the same width as the distribution in the scattering plane. So while the present experiment measured a substantial portion (at least 40% for π^+) of the azimuthal proton yield corresponding to the angular range of accepted pions, integration over the azimuthal angle requires an extrapolation based on the assumptions of a Gaussian shape with the width set by the observed θ_p distribution.

The distributions for 105° and 127° show small tails at large proton angles. This same feature shows up in the data of Ref. 9 at all pion angles, where the tails are fit fairly well with Gaussians which are two to three times wider than the primary Gaussian. These tails are thought to be associated with the pion multiple scattering events.

A measure of the fraction of the inclusive cross section which comprises the $(\pi,\pi'p)$ reaction can be obtained by integrating the angular distributions, then integrating over ϕ_p, assuming that the distribution in ϕ_p is Gaussian with a width equal to that of the θ_p distribution, and taking the ratio to $d\sigma/d\Omega_\pi$, which is obtained by integrating the inclusive cross section over $T_{\pi'}$. Table II shows the cross sections and their ratios for the present experiment and for $T_\pi = 245$ MeV from Ref. 9. The ratios for the present experiment range from 30% to 55% and appear to vary

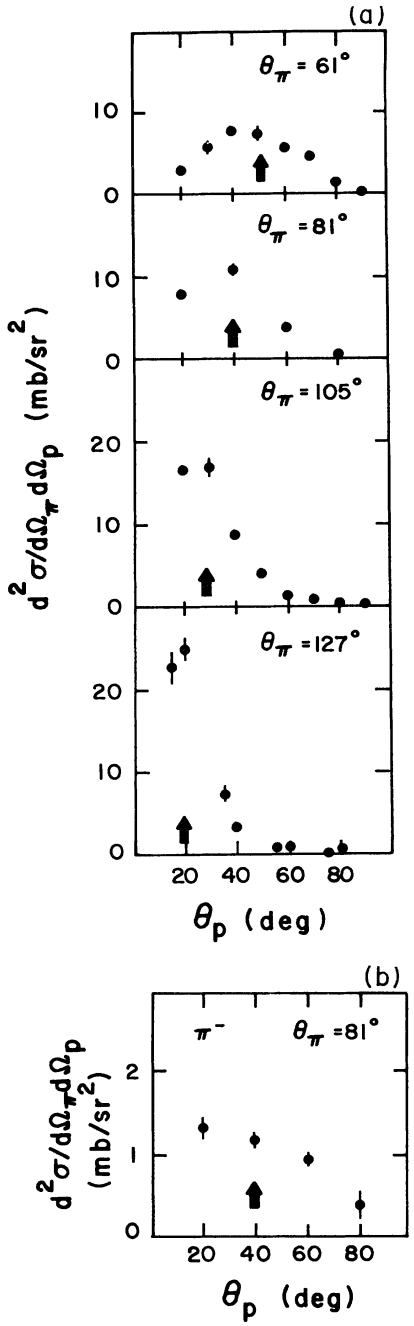

FIG. 8. The angular distributions in θ_p of the energy integrated coincidence cross sections for 220 MeV (a) positive and (b) negative pions incident on ^{12}C. The points here have been extrapolated from the data. The arrows indicate the elastic kinematics proton angle.

somewhat with the pion angle. The 245 MeV ratios[9] show a similar trend and magnitude. The differences between the 220 and 245 MeV ratios are not great enough to conclude that a significant energy dependence exists. The remaining part of the inclusive cross section may be attributed to the knockout of neutrons, deuterons, and possibly larger clusters, as well as to other processes such as pion production.

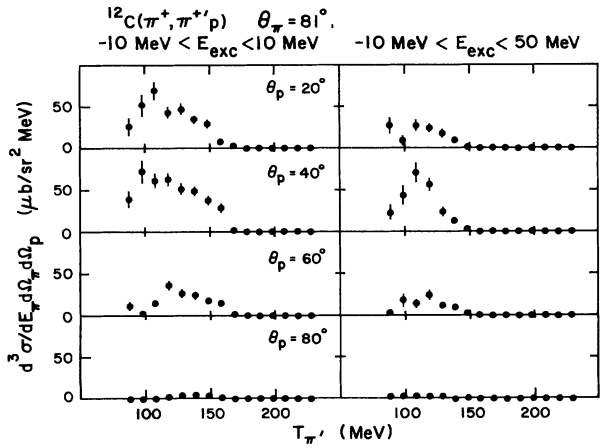

FIG. 9. The pion energy spectra obtained for 220 MeV π^+ incident on ^{12}C cut on low and high missing mass for $\theta_\pi = 81°$.

IV. DISCUSSION

The data already presented provide convincing evidence for the quasifree picture of pion knockout. At 220 MeV about one-third to one-half of the inclusive reaction can be attributed to the quasifree, $(\pi,\pi'p)$ process. The location and behavior with scattering angle of the peaks in the coincidence and proton energy spectra are also in accordance with this conclusion.

A. Missing mass cuts

It is of interest to ask how the coincidence energy spectra correlate with the excitation energy of the residual nucleus. Figure 9 shows the coincidence pion spectra with the cuts -10 MeV $\leq E_{exc} \leq 10$ MeV and 10 MeV $\leq E_{exc} \leq 50$ MeV (the "low missing mass" and "high missing mass" regions, respectively). Inspection of the low and high missing mass spectra reveals no obvious systematic differences.

The pion coincidence spectra of low and high missing mass for incident π^- are shown in Fig. 10. If these spec-

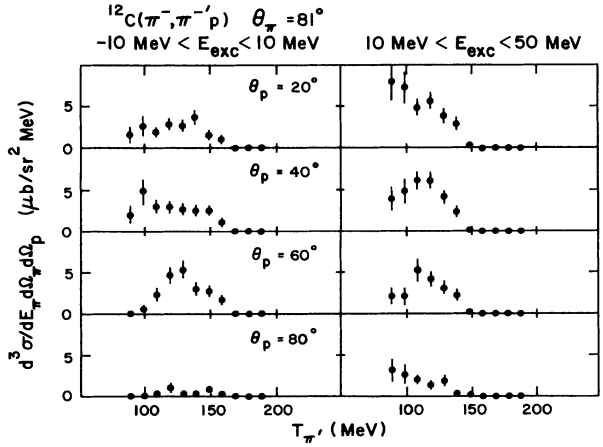

FIG. 10. The pion energy spectra obtained for 220 MeV π^- incident on ^{12}C cut on low and high missing mass for $\theta_\pi = 81°$.

TABLE II. Comparison of the integrated coincidence cross section with the inclusive (π,π') cross section.

T_π (MeV)	$\theta_{\pi'}$ (deg)	$(d\sigma/d\Omega)_{coin}$ (mb/sr)	$(d\sigma/d\Omega)_{incl}$ (mb/sr)	Ratio
π^+ incident:				
220	61	5.4 ±1.2	18.2±0.4	0.30±0.07
220	81	7.6 ±1.6	13.8±0.2	0.55±0.11
220	105	7.5 ±1.2	14.4±0.2	0.52±0.08
220	127	6.2 ±2.5	18.2±0.9	0.34±0.14
245[a]	70	6.4 ±0.8	13.4±1.1	0.48±0.07
245[a]	100	6.1 ±0.9	13.4±1.1	0.57±0.08
245[a]	120	8.7 ±1.0	14.5±1.2	0.60±0.08
245[a]	140	9.5 ±1.1	17.7±1.4	0.54±0.08
π^+ incident; low missing mass cut:				
220	61	3.8 ±1.0	18.2±0.4	0.21±0.06
220	81	4.0 ±1.3	13.8±0.2	0.29±0.10
220	105	3.2 ±1.0	14.4±0.2	0.22±0.07
220	127	4.8 ±2.0	18.2±0.9	0.26±0.11
π^- incident; low missing mass cut:				
220	81	0.41±0.70	11.2±0.2	0.04±0.06

[a]From Ref. 9.

tra are integrated over the scattered pion kinetic energies and plotted as a function of proton angle, it is found that the high missing mass angular distribution does not peak at the free π-p kinematics angle of $\theta_p=40°$, but rather at an angle forward of 20°. Furthermore, the distribution does not fall off very fast at large angles. In Table II the ratio of the integrated low missing mass cross sections to the inclusive cross section is about 0.04 with a large uncertainty. This is to be contrasted with the corresponding quantity for the π^+ case, where the ratio is about 0.25.

The angular distributions of the cross sections integrated over the low and high missing mass regions are shown in Figs. 11 and 12. The low missing mass entries in Table II show that the quasifree knockout events comprise about a quarter of the inclusive cross section and about half of all the knockout events for π^+. The remaining knockout events are the high missing mass cross section. The cross section ratio is rather more constant with a low missing mass cut than with a high missing mass cut. The tails in the 105° and 127° angular distributions of Fig. 8 are seen only in the high missing mass angular distributions of Fig. 11. This reinforces the idea that these tails are associated with events having pion multiple scattering and nucleon final state interactions.

B. Comparison of π^+ and π^- results

The inclusive energy spectra for incident π^- and incident π^+ have about the same magnitude as would be expected from the symmetry of the π^+N and π^-N interactions and from the fact that ^{12}C is an $N=Z$ nucleus. The coincidence spectra, on the other hand, are about an order of magnitude smaller for π^-. In fact, the ratio of the

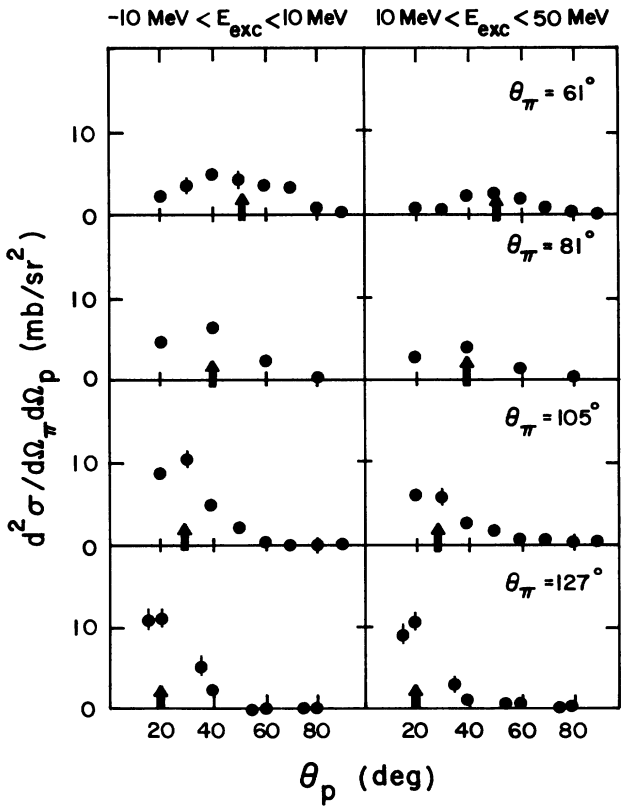

FIG. 11. The angular distribution in θ_p of the energy integrated coincidence cross section for incident π^+ cut on low and high missing mass. The points here have been extrapolated from the data.

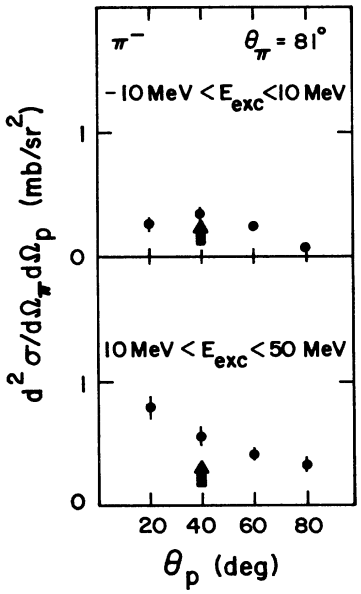

FIG. 12. The angular distribution in θ_p of the energy integrated coincidence cross section for incident π^- cut on low and high missing mass. The points here have been extrapolated from the data.

π^+p and π^-p elastic cross sections at $\theta_\pi = 81°$ is 8.0. This large difference between π^+ and π^- can be explained by assuming that most of the π^- inclusive yield comes from scattering on target neutrons while most of the coincidence yield comes from scattering on the target protons.

Table III shows the ratios of the π^+ and π^- inclusive and integrated coincidence cross sections. Only those parts of the π^+ spectra which overlap in energy with the π^- spectra are included in the ratio. The nuclear charge exchange model[15] (NCEX) predicts a ratio of 8 or less (depending on the charge exchange probability). The ratios for the low missing mass spectra at forward proton angles appear to be rather large in view of this model. The ratio is consistently largest at $\theta_p = 40°$, the conjugate angle.

TABLE III. Ratios of π^+ cross sections to π^- cross sections for $\theta_\pi = 81°$.

	$\theta_{p'}$ (deg)	Ratio
Inclusive		1.27±0.02
Coincidence	20	6.0 ±0.7
Coincidence	40	9.2 ±1.0
Coincidence	60	4.0 ±0.5
Coincidence	80	2.0 ±1.0
Low missing mass	20	16.9 ±3.2
Low missing mass	40	18.8 ±3.0
Low missing mass	60	9.6 ±1.4
Low missing mass	80	3.0 ±0.8
High missing mass	20	3.3 ±0.6
High missing mass	40	6.9 ±1.1
High missing mass	60	3.2 ±0.5
High missing mass	80	1.1 ±0.5

A comparison of the inclusive cross sections for π^+ and π^- as a function of scattered pion energy at $\theta_\pi = 81°$ [Figs. 2(b) and 5] shows that the ratio of the spectra is quite constant with energy, giving further evidence for the symmetry of the reactions on an $N = Z$ nucleus. However, the ratio here is not equal to unity as would be expected on the basis of the NCEX model and as has been observed in most other measurements of the inclusive cross sections.[5] Of the coincidence spectra ratios, those for $\theta_p = 40°$ are, on the average, the largest. This is the conjugate angle for $\theta_\pi = 81°$, and one would expect that the reaction would be most quasifree for the π^+; the preponderance of the nonquasifree events seen for the π^- would result in a smaller effect on the yield relative to the π^+ case.

A striking difference between the π^+ and π^- missing mass spectra is seen in the much larger proportion of the π^- events that are found in the high missing mass region. This and the peculiarities of the π^- angular distributions already noted both indicate that the coincidence events for incident π^- contain a much larger proportion of nonquasielastic events. In fact the number of high missing mass events is more than half of the total number of coincidence events.

A recent theoretical paper by Hirata *et al.*[16] examines the effect of the Δ-N interaction in the nuclear medium on pion reactions within the delta-hole model. Their results suggest that second order processes (which involve two nucleons) are enhanced for π^-p knockout reactions. This is particularly true near the minimum of the π-N elastic cross sections (about $\theta_\pi = 85°$ at 220 MeV) and at large momentum transfers. Furthermore, the interference between first and second order terms suppresses the π^-p cross sections at quasifree kinematics, so that the ratio between π^+ and π^- coincidence cross sections could be up to a factor of 2 larger than the quasifree ratio. This agrees well with what is seen for the low missing mass ratios in Table III.

V. CONCLUSION

In summary, this experiment provides evidence for the validity as well as the limitations of the quasifree picture of the $(\pi,\pi'p)$ reaction. For the reaction with incident π^-, the multiple scattering and nucleon final state interaction events are seen to dominate, although the quasifree cross section is still substantial. The kinematically complete measurement of the final particle momenta allows the clear separation of the knockout of the outer protons from other knockout reactions, thus clarifying the importance of the nonquasifree reactions. The data presented here will be useful in testing the assumptions used in the various theoretical models and for investigating secondary effects.

This work was supported in part by grants from the U.S. Department of Energy and the National Science Foundation.

*Present address: New Mexico State University, Las Cruces, NM 88003.
†Present address: Los Alamos National Laboratory, Los Alamos, NM 87545.
‡Present address: Technical Programming Services, P.O. Box 5247, Pleasanton, CA 94566.

[1]C. L. Morris *et al.*, Phys. Rev. C **17**, 227 (1978).
[2]S. B. Kaufman, E. P. Steinberg, and G. W. Butler, Phys. Rev. C **20**, 269 (1979).
[3]B. J. Lieb *et al.*, Phys. Rev. C **19**, 2405 (1979); **26**, 2084 (1982).
[4]Y. Ohkubo, N. T. Porile, and C. J. Orth, Phys. Rev. C **26**, 198 (1982).
[5]G. R. Burleson *et al.*, Phys. Rev. C **21**, 1452 (1980).
[6]S. M. Levenson *et al.*, Phys. Rev. Lett. **47**, 479 (1981).
[7]R. D. McKeown *et al.*, Phys. Rev. C **24**, 211 (1981).
[8]C. H. Q. Ingram *et al.*, Phys. Rev. C **27**, 1578 (1983).
[9]E. Piasetzky *et al.*, Phys. Rev. C **25**, 2687 (1982).
[10]L. W. Swenson *et al.*, Phys. Rev. Lett. **40**, 10 (1978).
[11]H. J. Ziock *et al.*, Phys. Rev. C **24**, 2674 (1981).
[12]E. Colton, Nucl. Instrum. Methods **178**, 95 (1980).
[13]SCATPI, a FORTRAN subroutine for calculating πN cross sections, described by John B. Walter and Glen A. Rebka, Jr., Los Alamos National Laboratory Report LA-7731-MS, 1979 (unpublished).
[14]J. A. Faucett, Ph.D. dissertation, University of Oregon, 1983.
[15]R. R. Silbar, Phys. Rev. Lett. **34**, 824 (1975); M. M. Sternheim and R. R. Silbar, Phys. Rev. C **24**, 574 (1981).
[16]M. Hirata, F. Lenz, and M. Thies, Phys. Rev. C **28**, 785 (1983).